Elsevier Editorial System(tm) for Construction & Building Materials
Manuscript Draft

Manuscript Number: CONBUILDMAT-D-10-01061R2

Title: Rehabilitation of masonry arches with compatible advanced composite material

Article Type: Special Issue: Masonry Research

Keywords: masonry; arch; strengthening; composite; TRM; tests

Corresponding Author: Ms Leire Garmendia, Ph.D

Corresponding Author's Institution: Tecnalia

First Author: Leire Garmendia, Ph.D

Order of Authors: Leire Garmendia, Ph.D; José-Tomás San-José, Ph.D; David García, Ph.D; Pello Larrinaga

Manuscript Region of Origin: SPAIN

Abstract: Stone masonry arches are structures of great functional and architectural importance as they may be found in a large number of constructions that are mainly historic buildings. Although relatively solid structures, time has taught us that environmental conditions, as well as their load history, use and possible accidents can lead to their collapse, all of which entails a risk of losing a large amount of our architectural and cultural heritage.
In this research work a compatible strengthening system for the rehabilitation of stone arches was investigated. The strengthening material was constituted of basalt textile embedded in an inorganic matrix known as Basalt Textile-Reinforced Mortar (BTRM) and provides an alternative to the usual reinforcement methods. The research work was based on an integral analysis of this reinforcement solution and its application to stone masonry. The first stage involved physical-chemical and mechanical tests to characterize the materials that constitute the masonry and the strengthening system. In the second stage, six arches were tested by means of displacement control up to the point of collapse. These arches were built according to different criteria: (1) dry or with mortar joints and (2) non-strengthened or strengthened on the extrados.
The experimental results obtained in this research work demonstrated good physical-chemical compatibility between the BTRM reinforcement system and the corresponding stone masonry substrate and validated its mechanical effectiveness for the reinforcement of arched structures in terms of load bearing capacity and ductility.

***Research Highlights**

1. Study of the compatibility and effectiveness of Basalt Textile Reinforced Mortar (BTRM) as strengthening material for arched masonry structures.
2. Integral characterization of individual materials and strengthening composite material.
3. Construction, strengthening and testing of masonry arches in laboratory.
4. Discussion of the results that validate the strengthening system.

Construction and Building Materials

Rehabilitation of masonry arches with compatible advanced composite material

L. Garmendia[a*], J.T. San-José[a,b], D. García[a], P. Larrinaga[a]

[a] *TECNALIA. c/Geldo – Parque Tecnológico de Bizkaia, Ed. 700, 48160 - Derio, Spain*
[b] *University of the Basque Country, Dept. of Engineering of Materials. c/ Alameda Urquijo s/n, 48013 Bilbao, Spain*

* *leire.garmendia@tecnalia.com, TEL : + 34 94 607 33 00 ; FAX +34 94 607 33 49*

ABSTRACT

Stone masonry arches are structures of great functional and architectural importance as they may be found in a large number of constructions that are mainly historic buildings. Although relatively solid structures, time has taught us that environmental conditions, as well as their load history, use and possible accidents can lead to their collapse, all of which entails a risk of losing a large amount of our architectural and cultural heritage.

In this research work a compatible strengthening system for the rehabilitation of stone arches was investigated. The strengthening material was constituted of basalt textile embedded in an inorganic matrix known as Basalt Textile-Reinforced Mortar (BTRM) and provides an alternative to the usual reinforcement methods. The research work was based on an integral analysis of this reinforcement solution and its application to stone masonry. The first stage involved physical-chemical and mechanical tests to characterize the materials that constitute the masonry and the strengthening system. In the second stage, six arches were tested by means of displacement control up to the point of collapse. These arches were built according to different criteria: (1) dry or with mortar joints and (2) non-strengthened or strengthened on the extrados.

The experimental results obtained in this research work demonstrated good physical-chemical compatibility between the BTRM reinforcement system and the corresponding stone masonry substrate and validated its mechanical effectiveness for the reinforcement of arched structures in terms of load bearing capacity and ductility.

KEYWORDS: masonry, arch, strengthening, composite, TRM, test.

1. Introduction

Masonry structures form part of our architectural heritage. Their presence in our everyday life is such that we tend to regard them as quintessential elements in our landscape. Indeed, it is difficult to imagine the built environment without these structures. Furthermore, they often comprise masonry arches that are essential to a large number of buildings, many of which are historic and all of which are of great functional as well as cultural importance: housing, religious buildings, bridges, footbridges, aqueducts, and waterways, among others.

Arches are building artefacts made of voussoirs which are placed in a specific curved form in order to stand over the empty spaces beneath them. Their stability is achieved by simple gravity force, which means that they work only under compression. As well as their spectacular design, they are impressive because of their capacity to adapt to movement in their supporting structures and to withhold greater loads than foreseen, opening and closing cracks that are not in themselves harmful to the structure until a number of hinges are formed which convert the arch into a mechanism.

Therefore, in view of the need to conserve the heritage inherited from earlier generations and the fact that this activity is supported by investment policy that targets restoration works (in Spain, government plans for 2009-2012), the importance of an in-depth study of effective and feasible restoration methods and solutions that are applicable to masonry structures becomes apparent. The main challenge resides in further development of new techniques, materials and reinforcement processes that will lead to the discovery of alternatives to the more traditional solutions, which are incompatible in certain scenarios (technical-cultural incompatibilities).

However, masonry structures have, until recently, largely been ignored as an area of interest for structural researchers. In this context, poor knowledge of masonry structures, assessment methods and reinforcement techniques should be acknowledged in comparison with other construction materials.

Masonry arches can be damaged due to inadequate design, poor construction practices, changes in their use, ageing effects, poor maintenance, fatigue effects, foundation settlement, earthquakes, architectural changes or load increments. As a consequence, it is important to evaluate the structural

safety of the building and later, if so required, to design a reinforcement solution. Effective reinforcement restores structural performance, increases load capacity and prevents brittle collapse. Conversely, reinforcement is also necessary in the cases where the structures must satisfy the requirements of current codes and standards. Coupled with concerns over the maintenance of our architectural heritage, there is wide interest nowadays in studying new strengthening techniques in greater detail.

Prior to applying the reinforcement, all possible solutions must be studied, giving special consideration to their efficacy and compatibility. Conventional reinforcement techniques (saddling, shotcrete sprayed onto the intrados, etc.) can be difficult to use and they introduce new rigid and resistant structural elements which increase the applied load and change the natural structural behaviour of the building.

In the past few years, new reinforcement materials used in other applications, such as aeronautics, have been introduced to the world of restoration. These materials have, on the whole, been presented in the form of Fibre-Reinforced Polymers (FRP), which are made up of synthetic fibres embedded in resins. To date, the most widely used FRP, by reason of its mechanical advantages and despite its high cost, is made of carbon fibres embedded in an epoxy resin.

The possibility of adopting FRP composites for the strengthening of masonry was initially investigated by Croci in 1987 [1]. Over the past two decades, great interest was devoted to the reinforcement of arches and vaults using FRP materials and several experimental works show that it is a valid option for the strengthening and/or repair of masonry [2, 3, 4, 5, 6] and, particularly, arched masonry structures [7, 8, 9, 10]. However, several drawbacks of the FRP must be underlined as narrow working temperature range , high cost, inability to apply FRP on wet surfaces, its fragility, etc. Moreover, in many heritage cases, epoxy resins are totally forbidden for their incompatibility with substrates.

In the case of structures with an arch shape, reinforcement can take place in different ways in order to avoid hinge formation. It can be applied to the external as well as to the internal surface of the arch (or to both) and it can also be a continuous reinforcement of the whole surface [7, 8, 11, 12, and 13] or a partial reinforcement [14] if it only covers those areas that can be considered as most critical. This last option only shifts the position of the hinge formed rather than avoid it. Tests have also been carried out on arches reinforced with FRP strips that are anchored with spike anchors made of the same material [15, 16, 17]. However, the influence of the different strengthening layouts on the structural behaviour is not entirely clear. There is no consensus about which strengthening layout provides the highest increase in the collapse load or the best ductility behaviour [17,18].

With the objective of providing a solution to the physical-chemical incompatibilities that FRP presents [19] when applied to masonry, alternative reinforcement solutions must be studied, as is the case of the Textile Reinforced Mortar (TRM) covered in this research project.

TRM comes from substituting an organic matrix with an inorganic matrix. This could be a mortar, either cement-based (where the use of cement is acceptable) or a local non-cement based mortar compatible with the specific materials used in each work. This new material seems to be a promising solution for strengthening masonry structures as its main properties are: water-vapour permeability which makes it compatible to be applied on masonry, appropriate for use over a humid substrate, it does not emit toxic substances, therefore, it does not require the use of special equipment, it is easy to manipulate, it is applicable over irregular deteriorated surfaces, such as a levelling material, without the need of a specific treatment, thus reducing the number of weak joint interfaces, it is fire resistant and it does not need specialized labour.

A further issue is that, when mortar is used as a matrix of the composite strengthening system, the fibres should be in a textile instead of a fabric form, as in polymer matrices, in order to guarantee adhesion between the matrix and the strengthening core. Moreover, an appropriate textile must be found (entirely compatible) with good physical-chemical characteristics.

The basalt fibres have not been extensively used in FRP, despite presenting similar mechanical properties to glass at a much lower cost than carbon or aramid, which makes them very appropriate for low-cost interventions. Furthermore, some research groups have demonstrated better results for ultimate resistance and global ductile behaviour when the arch is reinforced with glass FRP as opposed to carbon FRP [6]. As a consequence, it seems logical to think that basalt fibre textiles will work adequately in the inorganic matrix.

The specific tenacity (ratio: rupture stress/density) of basalt fibres greatly exceeds that of steel fibres. Basalt is roughly 5% denser than glass. The elastic tensile modulus of basalt fibres (82-110 GPa) is higher than that of E-glass fibres (70-75 GPa). Basalt fibres show excellent natural adhesion to a broad range of binders, coating compounds and matrix materials in composite applications [20]. It results in fabrics with high levels of dimensional stability that exhibit reasonable suppleness, drape ability and good fatigue resistance. Basalt is non-toxic, completely inert and without any environmental restriction. Because of its

thermal insulating properties, they are ideally suited for use as fire-protection applications. All these properties mean that basalt fabrics are an attractive option for composite strengthening [21, 22].

2. Objective

As a consequence of the existing problem presented, an in-depth study of a reinforcement system for the restoration of stone arches has been conducted within the framework of this research work. It seeks to contribute to a broader knowledge on the behaviour of stone arches and the effectiveness of a innovative reinforcement system based on basalt textile embedded in inorganic matrices (mortar modified with polymers) known as Basalt Textile-Reinforced Mortar (BTRM). It must be a compatible, minimally invasive, easy to apply and cost effective strengthening solution for stone masonry arches.

As a first step, material characterization was carried out. The physical-chemical properties allow the obtaining of data for determining the compatibility between the materials that make up an arch and those used for its reinforcement; while the mechanical properties of the materials allow the determination of the resistance parameters and the behavioural laws.

As a second step, the experimental work on masonry arches (constructed with materials and geometry present in real structures) was designed in order to fulfil the following objectives: to characterize the structural behaviour of non-strengthened arches and study the influence of the strengthening system on the behaviour of the arches as it relates to the failure mode, resistive capacity and deformation and to contribute to wider knowledge of the behaviour of strengthened arched masonry structures.

3. Material Characterization

This section is aimed at the chemical, physical and mechanical characterization of every material used in this research project.

The arches were built using stony material known as Arenisca de Aguilar sandstone extracted from the quarry at Quintanilla de las Torres, in the province of Palencia (Spain). This stone is currently used for substitutions in real interventions.

The composition of the mortar used for setting the voussoirs was adjusted in line with the characteristics of mortars commonly used in ancient masonry structures. The correct proportions were established by gathering data from the specifications of ancient mortars, which were determined at TECNALIA from real life studies.

With regard to the strengthening material, it is based on basalt textile embedded in a pozzolanic mortar matrix (Basalt Textile-Reinforced Mortar-BTRM). The type and quality of mortar used in the reinforcement are extremely important and crucial to the life of a stone building. A cement-free matrix mortar is therefore used (Mape-Antique Strutturale). Furthermore, a cement-free base mortar (Mape-Antique Rinzaffo) was applied in order to improve adhesion and add chemical/physical resistance to soluble salts of macro-porous dehumidifying mortars. Both are pozzolanic mortars modified with polymers, supplied by IBERMAPEI. Apart from the excellent physical-chemical properties of basalt, there are three main reasons why this mineral fibre was selected:

1. As discussed before, masonry structures need reinforcements which are not too rigid and can adapt to the high deformation they are subjected to. Basalt fibres show similar properties to those of glass fibres with a slight improvement, which makes them very suitable for these applications.
2. They are easy to obtain and therefore have a low cost.
3. They are ideal for use with mortar.

The bitumen-impregnated basalt textile used in this research is supplied by FYFE Europe. The manufacturing specifications are presented in Table 1:

Table 1. Technical specifications of the basalt textile used in this research

3.1. Physical-Chemical Analysis

The petrographic analysis (see Figure 1) shows that the rock has fine evenly-sized grains and presents medium to low cohesion and a low degree of compaction. It is composed of 65% quartz in which white grains predominate alongside reddish veins. The sandstone is a uniform, fine-grain, yellowish-grey sandstone rock with light rose-coloured tones, somewhat weak to the touch. The rock could be classified as sub-arkose [23], i.e., a sandstone rock with less that 15% of sandstone matrix, very rich in quartz and with less than 25% of feldspar in the weft.

Figure 1. Petrographic analysis of the sandstone. Macroscopic (left) and microscopic (right) photographs

The jointing mortar is made of lime, white cement, sand and water, in volume proportions of 0.5, 2, 10 and 4, respectively. Given that lime mortar takes a lot longer to reach the necessary mechanical strength, in some cases one can speak of centuries, it was considered necessary to add white cement so that the strength of the mortar would increase at an earlier age. It is used to fill the joints and its purpose is to stop the passage of water, regularize the seating between blocks uniformly distributing the load and, finally, to transmit the stress.

The mineralogical analysis of the materials was carried out using the X-ray diffraction technique. The diffractometric measurements were taken using a Philips X'Pert Pro MPD pw3040/60 diffractometer equipped with a copper ceramic tube. The instrument conditions at the time of taking the measurements were continuous 2 to 75° 2Θsweep, 40kV, 40 mA generator current for one hour. The analysed sample was ground and homogenized automatically in an MM301Retsch mixing grinder in order to process it adequately. The results are presented in Table 2 and 3. Black dots indicate the relative abundance of the mineral in each specimen.

Table 2. Mineralogical characterization of the stone and jointing mortar

The mortars that composed the strengthening system are two: a base mortar named Mape Antique Rinzaffo for surface preparation and a matrix mortar Mape Antique Strutturale, where the textile is embedded. Both are pozzolanic mortars modified with polymers.

Table 3. Mineralogical characterization of strengthening mortars

In addition to the mineralogical characterization, the parameters presented in Table 4 were all determined for each material based on current standards: capillarity absorption (UNE-EN 1925:1999 and UNE-EN 1015-18:2003), absorption under atmospheric pressure (UNE-EN 13755:2002), water vapour permeability (UNE-EN 1015-19:1999) and porosity, average pore size and distribution of pore sizes by means of mercury porosimetry (ISO 15901-1:2007).

Table 4. Physical analysis of the materials

3.2. Mechanical Analysis

The mechanical analysis was performed on the constitutive materials of the arches and the strengthening, as well as on the composite strengthening material by means of tensile tests.

3.2.1. Stone and mortars

Compressive strength tests on ten stone specimens were based on Standard UNE-EN 1926:2007. The value of the elastic modulus was calculated on three specimens in accordance with Standard ASTM C 469:2002 while the indirect tensile strength (Brazilian method) was carried out on five specimens following the specifications stated in Standard UNE-EN 22950-2:1990.

Regarding the different type of mortars, the samples were taken directly during the construction and strengthening of the arches and were stored at room temperature and at a controlled relative humidity (20 ºC and HR 60%). Subsequently, compression and flexotraction tests on three specimens each were performed as per standard UNE-EN1015-11:1999. The modulus of elasticity was obtained following Standard ASTM C 469:2002. Results of average compression value (f_{cm}), tensile strength (f_{tm}) and elastic modulus (E) are presented in Table 5.

Table 5. Average values for mechanical test results of materials

3.2.2. Basalt Textile

The textile has been characterised in laboratory by means of uniaxial tensile tests, varying the amount of rovings, as presented in Figure 2. The standards relating to the testing of similar products were consulted prior to the characterization of this textile. However, no explicit regulations or recommendations for testing mineral fibres woven as a mesh are available. On the whole, 40 specimens of between 400 – 500 mm long were tested in accordance with internal procedure which was based on

Standard ASTM D5034. One (TL 1), two (TL 2) and four (TL 4) roving specimens tested in longitudinal directions and four (TT 4) roving specimens in transversal direction were tested. The testing machine displacement rate was 5mm/min.

Specimen TL-1 Specimen TL 4 Specimen TT 4

Figure 2. Pure tensile tests of several basalt textile specimens

A comparison between the average values of the total load bearing capacity in different units (f_f, σ_f), elongation at the ultimate load ($e(f_f)$) and the elastic modulus of fibres (E_f)obtained for the different type of specimens is shown in Table 6.

Table 6. Textile tensile test results

During the tests, fibres started to absorb the load slowly up until all the strands are aligned. From this point on, the load was distributed among all the strands and the load absorption increased quicker and in a linear manner. When the rovings started to break, the load decreased rapidly.

Having eliminated those specimens from the results that were spoilt or that had breaks near the ends, a scatter in the results was noticeable (around 10%). This scatter is explained by the processing of the fibres and the manufacture of the textile. In all cases, the development of the deformation and the failure mode are significantly affected by the practical impossibility of providing the same initial length and load to each one of the thousands of fibre strands that compose the textile. The fibres that had been subjected to greater traction were the first to break.

Comparing the results obtained in the case of one and two roves, the increment in the ultimate resistance of the specimen is approximately proportional to the number of roves; nevertheless, this not the same for a larger number of roves. In the specific case of the TL4, the ultimate resistance is 24% less compared to the ultimate resistance of the specimen with a single strand. It seems logical to think that the ultimate load of a specimen with four roves would be four times the load of a specimen with a single strand, under similar failure modes if there were no peculiarities that would make the pull non-homogeneous. On the other hand, one must highlight the fact that the failure on the specimens type TL4 has occurred close to the clamps in the majority of cases, probably due to the stress concentration. Therefore, it can be assumed that the actual tensile strength of the specimens is higher than that recorded.

It can also be noticed that in the longitudinal direction presents a slightly greater resistance compared to the perpendicular one, which in this case is around 33% larger. This could be due to the greater quantity of textile in the longitudinal direction.

Regarding the deformation elastic modulus (E_f), the single-strand specimens (TL1) have a higher modulus value, which would imply a more rigid behaviour of the specimens. This can be attributed to the fact that in a single-strand specimen it is easier for all the fibres that make it up to be pulled simultaneously. The value of the modulus is closer for the two-strand (TL2) and four-strand (TL4) specimens. In the case of specimen with four roves in the transversal direction (TT4), the value of the modulus in smaller, which implies a bigger deformability of the specimens due to the lesser number of fibres.

3.2.3. Textile reinforced mortar (TRM)

Regarding the textile reinforced mortar (TRM), the understanding of the cracking process is of crucial importance at the time of calculating load-bearing capacity, deformation behaviour and limiting values in order to design serviceability. Cracking distance and crack width are determined not only by the stress but also by the bonding action between the textile reinforcement and the mortar matrix.

With the purpose of analysing the BTRM tensile behaviour, specimens of 100 x10 mm^2 cross-sectional area and 600 mm in length were prepared.

The specimens were built with two layers of basalt textile which were embedded in Mape-Antique Strutturale mortar. In order to promote the failure of the specimen in its middle third portion, the ends of the specimen were reinforced with two additional layers of 200 mm x 100 mm textile. After their construction, the specimens were kept for 7 days in a damp chamber (20ºC and 100% RH) and later on, in a controlled environment (18 ºC and 60% RH) during 28 days of curing time.

There were two variables related to the gripping system of the textile. Firstly, ten specimens (TRMA) were tested where the gripping devices compressed the compound material, which was impregnated on the exterior with an epoxidic resin in order to prevent slippage. Afterwards, seven additional specimens (TRMB) whose two textile layers had an excess length of textile on its ends were tested. In this case, the gripping device compressed not only the compound material but also the excess textile, preventing the slippage between the textile and the mortar. This latter test was carried out with the objective of replicating better the working conditions of the reinforcement above the arches. At the time of testing the

reinforced structures, a slippage between the mortar and the textile could not be observed until the point of collapse. Tests (see Figure 3) were carried out using a speed of 0.5 mm/min. The strains within the measurement range were recorded with four *Linear Variable Displacement Transducers* (LVDTs), two on each side.

Figure 3. Preparation and testing of the TRM specimens

Figure 4 presents the results obtained for TRMA specimens.

Figure 4. Textile stress-strain curves: two-ply specimen (TRMA) tensile tests – 0.5 mm/min

The stress-strain curve is characterized by three very different stages. In Stage I, the specimens show a very rigid behaviour where loads are absorbed with very little deformations. This phase ends with a load decrease due to the cracking of the matrix. In Stage II, the specimen recovers the load linearly and its behaviour is basically influenced by the mechanical properties of the textile. The width of the cracks grows due to the delamination between fibres and mortar, and leads to a loss of the tension stiffening effect. However, the transversal fibres oppose the resistance so that the load can continue to increase. At the time of reaching the ultimate strength, the fibres fail partially, the second phase ends and Stage III starts with a sudden loss of mechanical capacity. Some of the specimens suffered large deformations due to the lack of adherence between the internal strands and between the textile and the matrix.

In reference with specimens type TRMB, the test speed was reduced to 0.3 mm/min for the purpose of being able to better appreciate the specimen's response to the load application. The results obtained are presented in Figure 5.

Figure 5. Textile stress-strain curves: two-ply specimen (TRMB) tensile tests – 0.3 mm/min

In this case, opposed to TRMA, delamination was prevented as failure happened due to breakage of the whole section. The stress-strain graphs obtained are characterized by the presence of two stages. In Stage I, even though small fissures appear, the slope is linear up to the point where the ultimate load is reached, with the exception of specimens TRMB-1, TRMB-3 and TRMB-5 which are characterized by showing an initial more unstable area, with small load losses caused by the appearance of cracks. The composite behaviour in this stage is influenced mainly by the properties of the textile. The value of the Young's modulus is higher than that of the textile. In Stage II, which starts after reaching the ultimate load, the graph shows small load oscillations caused by the failure of the strands at specific points. The stress is transmitted from one strand to the other until the whole section fails. A picture of the test is presented in Figure 3.

4. Arch Construction

A total of six arches were built with the following dimensions: 1130 mm span, 440 mm height, 250 mm depth and 120 mm width (see Figure 6). Three non-strengthened arches (type A) and three strengthened on the extrados (type EX). This strengthening solution was chosen because, often, the visible side of historic structures (the lower surface) cannot be changed.

With a view to reproducing the stone arches present in the existing heritage with the highest possible precision, the structures were built by expert builders from the Santa Maria de la Real Foundation, which among its other activities is active in the restoration of masonry structures. According to existing bibliography [24], the selected geometry accomplishes the existing arch typologies in Northwest Iberian Peninsula and can be classified as semi-shallow short span arch type. Furthermore, they also accomplish with the rise/span ratio established by Russian and German Engineers for arch bridges [25].

Figure 6. Geometry of the arches

With the objective of studying the way in which the mortar influences the masonry, one of the non-strengthened arches (A1) was built without mortar as opposed to the other two (A2 and A3) that were built using lime mortar joints. The rest of the arches had a small amount of mortar (around 5 mm thickness) for setting the joints, which is the most common case in the north of Spain.

Previous studies have demonstrated that, rather than preventing hinge formation, the use of non-continuous strengthening strips [14] simply displaces the points at which the hinges form. Moreover, the load-bearing capacity and the deformability of the structure are better in those cases where the

strengthening strips are continuous throughout the length of the arch. It was therefore decided to apply a continuous strengthening layer to the entire surface.

The basalt textile in use is bi-directional. The presence of transversal filaments was not justified as there were no loads in that direction, but they did help to improve fibre-matrix adherence and its adaptation to the form of the structure. Moreover, with the objective of increasing the capacity of the strengthening system, it was decided that two layers of textile would be applied.

The strengthening system was composed of a first layer of the cement-free Mape-Antique Rinzaffo base mortar and a second layer of cement-free Mape-Antique Strutturale matrix mortar, where the two layers of basalt textile were embedded. The cells of this mesh were displaced in relation to the cells of the first layer so that the longitudinal rovings of both meshes were distributed uniformly over the surface of the arch.

Previous research works propose the use of anchors to improve the adherence between the textile layers and the arch [14, 15, 16]. As a consequence, spike anchors were placed in the three arches in alternative voussoirs (see Figure 7). They consist of a threaded basalt yarn inserted into a pre-drilled hole in the stone that is filled with commercial grout. Half of the length of the spike anchor was introduced in the stone, the other half that was outside the stone, grabbing the basalt layers. Finally, a last layer of matrix mortar is applied. The mean thickness of the strengthening system was 15 mm.

Figure 7. Spike anchors location (left) and strengthening of masonry arch (right)

This experimental work has been designed in order to fulfil the following objectives:

- To characterize the structural behaviour of non-strengthened arches and arches strengthened with BTRM, which are tested by means of displacement control up to failure.
- To study the influence of the strengthening system on the behaviour of the arches as it relates to the failure mode, resistive capacity and deformation.
- To contribute to wider knowledge of the behaviour of strengthened arched masonry structures.

5. Arch Testing

The tests were performed on the TECNALIA platform for structural testing. The load was applied at the quarter of the span (see Figure 6), distributed along the whole of the upper surface of voussoir number 5, in order to facilitate the collapse of the structure. The tests were carried out up to collapse, using displacement control, at a speed of 0.12 mm/min. The arches were tested on a metal frame in order to provide them with a rigid support.

Both the horizontal displacement as well as the vertical displacement of alternate voussoirs were recorded during the test using LVDTs. Likewise, displacement outside the vertical plane of voussoir 8 and the stability of the abutments were registered. Finally, in order to monitor the verticality of the applied displacement more closely, instruments were set up to record any possible rotation of voussoir 5. In total, 14 displacement meters were used. The applied load was measured using load cell. Regarding data acquisition, the software MGCpluc with an indicator and control panel AB22A/AB32 from HBM were used. Data was recorded at a frequency of 10 Hz.

During the tests, continuous visual inspections were carried out for the control and recording of fissures, formation of hinges, failure modes, behaviour, etc.

5.1. Non-strengthened Arches

An arched masonry structure is stable under a given load condition provided that the thrust line, which represents the internal forces at every cross-section, is kept inside the central core (central third of the thickness). When the thrust line moves outside the central core, the formation and consequent opening of a crack takes place and a plastic hinge is formed. The appearance of successive hinges forms a mechanism that triggers the collapse of the structure [26]. The failure of the arch takes place when four hinges are formed.

Figure 8 presents the results obtained for non-strengthened arches. The data recording rate allows a precise analysis of the structure behaviour. However, in order to facilitate the comprehension of the global behaviour by means of a smoother curve, the polynomial regression curves are also presented. Moreover, the post-peak behaviour has been omitted as the comparison among the three arches from this point on is no direct.

Figure 8. Load-Displacement of load application point for non-strengthened arches

In the case of arch A1 (built without any mortar), the load was progressively applied until it reached the maximum value of 0.98 kN. The failure was characterised as sudden and without large deformations compared to strengthened arches (presented later on).

Arch A2 and A3 underwent load swings as a result of the settlements of the voussoirs due to irregular crushing of the jointing mortar.. After reaching the ultimate load (1.3 kN and 1.45 kN, respectively), failure was brought about by the formation of four hinges that turned the structure into a mechanism. From this stress-strain stage, it does not seem adequate to do an analysis or comparison between the samples, as they are already converted into a mechanism.

Figure 9 compares the displacements measured by means of LVDTs in the right haunch (load application point) and left haunch (opposite point). The loss of load corresponds with settlements due to jointing mortar crushing (as the deformation of the voussoirs is neglected) while the increase means that voussoirs are together again and the load is recovered. These settlements are registered in all voussoirs. As it is evident, the load causes also the displacement of the voussoirs located on the left haunch but with higher magnitude than the load application point, as the small movements of the voussoirs located in between are added.

Figure 9. Comparison of the displacement of the left and right haunches

The hinge-formation points were the same for arches A1 and A2. In the case of arch A3, the location of the hinge that formed on the opposite side of the load showed a slight variation. The order of appearance of the hinges is the same for arches A1 and A3 (see Figure 10).

Figure 10. Location and order of appearance of the hinges on non-strengthened arches

5.2. Arches strengthened on the extrados

The initial rigidity of the arches was similar in the three cases (see Figure 11). However, starting from an approximate displacement of 6 mm, each of the structures performed in different ways due to hinge formation at different locations, sliding between voussoirs or crushing of the stony material. As a result, a comparison of the structures behaviour is not appropriate. The value of the ultimate load of Arch EX1 is 19.3 kN; EX2, 16.83 kN and EX3, 12.65 kN.

Figure 11. Load/Displacement of load application point for arches strengthened on the extrados

It was observed that the strengthening system in arches EX1 and EX2 delayed hinge formation on the intrados of the arch. In the case of EX1, although a slight sliding at the keystone was also observed, failure was caused by breakage of the BTRM in the area under tensile stress, whereas in the case of EX2, the collapse was caused by debonding of the strengthening system under a smaller load than in the former case. In the case of arch EX3, collapse was caused by crushing of a voussoir that had been weakened at its source of origin, although it was possible to observe the improvement of the arch's overall strength, as it was capable of maintaining a 10 kN of load at its plateau.

Figure 12 presents the location and order of formation of the hinges on the arches. In some cases, it was not possible to determine the order of appearance of the hinges because final failure occurred suddenly.

Figure 12. Location and order of appearance of the hinges on arches strengthened on the extrados

In EX 2 (see Figure 13), the anchor placed at voussoir 13 prevented the strengthening strip from debonding as well as at the right abutment where, despite the slight delamination, the anchorage maintained the strengthening bonded up until the end of the test. It is worth mentioning that, on the contrary, the anchor embedded at the left abutment was completely extracted, probably because of the normal stress on the surface or due to an inappropriate setup.

Figure 13. Detailed photographs of arch EX2

6. Discussion of Results

6.1. Physical-chemical analysis

The physical-chemical characterization of the stone and the reinforcement mortars described in sub-section 2.1 has demonstrated that they have the same stony nature based on silicon arids. Small pores are

predominant in the stone, which facilitate absorption by capillarity and decreases the absorption capacity of water at atmospheric pressure. In the base mortar there are two pore sizes, with a higher concentration of the bigger typology. In the matrix mortar, the pore concentration is higher, but its size is smaller than that found in the base mortar. Regarding permeability to water vapour, both mortars have similar magnitude values. Therefore, it becomes evident that the stone is less porous than the reinforcement mortar; the latter allows the flow of humidity through its cavities and stops the accumulation in the interface stone (ashlar stone)-mortar and, therefore, stops the loss of bonding by powdering of the rock or salt-formation phenomenon. That way, compatibility between the reinforcement material and the rock is proven on the basis of the hydric properties.

6.2. Mechanical characterization of the strengthening composite material

As shown in sub-chapter 2.2.2 it is difficult to obtain perfect lining up of all the roves in the textile due to the manufacturing process, this can give rise to a heterogeneous distribution of the tension. When the first roving fails, a loss in the load takes place and the remaining stresses are redistributed. The impregnation of the textile helps to distribute the load between rovings in a more homogeneous way.

Moreover, tensile tests on the TRM presented in sub-section 2.2.3 have demonstrated that there is no complete utilization of the mechanical properties of the textile. This utilization is reduced to half its capacity, and is limited by the loss of adherence between the textile and the matrix and between the external and internal strands of the textile what provoked delamination. In the case when slippage can be stopped physically (as in TRMB tests type), the use of the mechanical capacity of the textile increases up to 75% and the global behaviour of the TRM is more rigid. This slippage between textile and matrix is a possible failure attributed to this type of material, which has been made evident in other works [27]. The adherence could also be improved by increasing the length of the specimens so that delamination is avoided. For instance, in the arch testing which is going to be presented later on, loss of adherence was not appreciated up until close to failure moment. This could be due to the fact that the bonded length is enough to prevent delamination between fibres and matrix.

In order to obtain a good performance TRM, an affinity has to exist between the textile and the matrix. Mortar with small grain sizes, adequate fluidity to impregnate the fibres and good bonding, can provide the adequate resistance properties to the TRM. The impregnation between the textile and the matrix requires especial care as the bonding properties depend on them. Moreover, as presented also by other authors [28], the final properties of the TRM will be a function of the geometry of the textile: bidirectional textiles improve the stability of the knots and the resistance to the traction capacity of the matrix, as well as its modulus of deformability.

6.3. Arch testing

As a summary of the data registered by the 14 LVDTs, the movements recorded during the tests are: a) descent of the loaded semi-arch; b) rise of the unloaded semi-arch and c) horizontal displacement to the unloaded semi-arch. The lack of a setting mortar in arch A1 gave rise to a more continuous deformation of the structure. It was observed that the mortar in arches A2 and A3 allows the structure to adapt to the new load conditions to which it was subjected, causing the firm setting of the voussoirs and therefore, occasional loss of contact between the load application points and the structure. Arches A2 and A3 showed a similar behaviour in terms of rigidity. With respect to the hinge position, due to its proximity, it may be considered to have formed in the same area in all cases. The small difference can be caused by heterogeneities inherent to the masonry or by slight geometric variations introduced at the time of its construction. On the other hand, the order of appearance of hinges was different for arch A2, probably due to the sliding of its keystone in relation to its central positioning. This fact gave rise to the closure of the initial separation between voussoirs 11 and 12 and to the formation of the hinge between voussoirs 10 and 11 in the last instance.

Table 7. Summary of experimental test results

Regarding the tests carried out on strengthened arches, the experimental data showed a considerable increase in the resistive capacity of the arches strengthened along their external surface (see Table 7), 13 times larger compared to the non-strengthened arches. Likewise, a higher degree of structural ductility was observed as it was 3 times higher than non-strengthened arches.

This strengthening system enables to predict the position of the future hinges beforehand due to small fissures present on the BTRM. However, the different failure modes observed (even though failure due to stone material weakness -EX3- is not considered) do not permit to establish a single failure mode for arches strengthened on the extrados, in absolute terms, which opens up further avenues to widen research in this field.

With reference to the spike anchors, the study of their effectiveness is a difficult task. The arch structures apparently remained unaltered up to the point where the hinges started to form, for which reason it was not possible to verify whether the anchors had any effect. Furthermore, it is difficult to guarantee the good execution of these anchorages, so after the tests, the quality of execution was verified. It was observed that various anchors were pulled out from the voussoirs fairly easily. Nevertheless, there was no debonding of the strengthening strips in this area. This fact means that the reinforcement-substrate interface could be enough to ensure adherence between the two, without the need for anchors. However, a further in-depth study is being carrying out in TECNALIA in order to study this fact and the load transmission between the anchor and the substrate. Up until now, several single-lap shear test were performed on different type of specimens varying the bonded length and in most of the situations, failure occurred in the BTRM so it was not due to loss of adherence in the reinforcement-substrate interface.

7. Conclusions

The building and subsequent testing of the stone masonry arches reinforced with Basalt Textile Reinforced Mortar on the external surface has validated the simplicity of its application, particularly, to those that have a complex form (arches, vaults, etc.) and the effectiveness of this strengthening system as it notably improves the mechanical behaviour of the structure in terms of resistive and deformation capacity.

Furthermore, the cement-free mortars used provide physical-chemical compatibility with the stone substrate and prevent the substrate from tearing off, which is common in polymer-based reinforcements. These are very important properties for the conservation of historical heritage and it is a positive point if the strengthening has to be removed without ripping of the substrate.

Currently, basalt textile is one of the most ideal materials for application as the resistant core in the reinforcement of masonry structures due to its excellent properties; amongst these the following stand out: deformability, low cost and resistance to corrosion, high temperatures and humidity. It is also worth mentioning the competitive cost of this system compared to current reinforcement methods (the matrix is composed of an easy to obtain material and the basalt has similar price to glass fibre, it does not required specialized labour, etc.).

To conclude, BTRM is an effective solution in the reinforcement of stone masonry arch-shaped structures and it is a possible an alternative solution when the use of traditional strengthening system is limited.

Acknowledgements

This research work has been made possible thanks to financing from the Basque Government (TEXMOR-S-PE07LA09) and the Diputación Foral de Bizkaia (BIRGAITEK 7-12-TK-2009-10).

References

[1] Luciano R., Marfia S. and Sacco E. *Reinforcement of masonry arches by FRP materials: experimental tests and numerical investigations.* University of Cassino. 2002.

[2] Schwegler G. *Masonry construction strengthened with fiber composites in seismically endangered zones.* Proceedings of 10th European Conference on Earthquake Engineering, Vienna, Austria 1994.

[3] Saadatmanesh H. *Fiber composites for new and existing structures*. ACI Structural Journal 1994; 91, 346-354.

[4] Ehsani M.R. *Strengthening of earthquake-damaged masonry structures with composite materials.* In Non-metallic (FRP) Reinforcement for Concrete Structures. Ed. L. Taerwe; 1995, 680-687.

[5] Seible F. *Repair and seismic retest of a full-scale reinforced masonry building*. Proceedings of the 6th International Conference on Structural Faults and Repair 1995; Vol. 3, 229-236.

[6] Triantafillou T.C. *Innovative strengthening of masonry monuments with composites*. Proceedings of 2nd International Conference Advanced Composite Materials in Bridges and Structures, Montreal, Quebec, Canada. 1996.

[7] Valluzzi M.R. and Modena C. *Experimental analysis and modelling of masonry vaults strengthened by FRP*. III Int. Seminar on Structural Analysis of Historical Constructions (SAHC-2001), Guimaraes (Portugal), 7-9 November 2001, 627-635.

[8] Foraboschi P. *Strengthening of masonry arch bridges using advanced composite materials*. Composites in Construction, Figueiras et al 2001. ISBN 90-2651-858-7.

[9] Lissel S. L. and Gayevoy A. *The use of frp's in masonry: A state of the art review*. In Proc. International Conference on the Performance of Construction Materials, Cairo, Egypt; 2003, pp. 1243–1252.

[10] Oliveira D., Basilio I. and Lourenço P. *FRP strengthening of masonry arches towards an enhanced behaviour*. Bridge maintenance, safety, Management, Life Cycle Performance and Cost – Cruz , Frangopol & Neves (eds); 2006. Taylor & Francis Group, London, ISBN 0415403154

[11] Como M., Ianniruberto U. and Imbimbo M. *La resistenza degli archi murari rinforzati con fogli in FRP*. Proc. of Mechanics of masonry structures strengthened with FRP – materials. Venezia, Italy, 2006.

[12] Briccoli Bati S., Rovero L. and Tonietti U. *Experimental analysis on scale models of CFRP reinforced arches*. MuRiCo3 Conference, Meccanica delle strutture in muratura rinforzate con compositi. 22-24 April 2009, Venice.

[13] Jasienko J., Di Tommaso A. and Lukasz B. *Experimental Investigations into Collapse of Masonry Arches Reinforced Using Different Compatible Technologies*. MuRiCo3 Conference, Meccanica delle strutture in muratura rinforzate con compositi. 22-24 April 2009, Venice.

[14] Basilio I. *Strengthening of arched masonry structures with composite materials*. PhD Thesis. Escola de Engenharia Universidade do Minho, 2007.

[15] De Lorenzis L., Dimitri R. and La Tegola A. *Strengthening of masonry edge vaults with FRP composites*. Composites in Construction 2005. 3rd International Conference. Lyon, France July 11 – 13, 2005.

[16] Aiello M.A., De Lorenzis L., Galati N., and La Tegola A. *Bond between FRP laminates and curved concrete substrates with anchoring composite spikes*. Proceedings IMTCR'04, Lecce, Italy.

[17] Oliveira D., Basilio I. and Lourenço P.B. *Experimental behaviour of FRP strengthened masonry arches*. Journal of Composites for Construction. ASCE, May/June 2010, 312-322.

[18] Garmendia L. *Rehabilitation of masonry arches by a compatible and minimally invasive strengthening system.* Doctoral Thesis. Escuela de Ingeniería de Bilbao, 2010.

[19] Garmendia L., San-José J.T., García D., Larrinaga P., San-Mateos R. and Díez J. *Experimental study on masonry arches strengthened with textile-reinforced mortar*. Structural Faults & Repair 2010. Edinburgh. ISBN 0-947644-67-9.

[20] OPERHA. *Open and fully compatible next generation of strengthening system for the rehabilitation of Mediterranean building heritage*. Contract nº: 517765 (INCO), 6th FP; 2006-2008.

[21] García D. *Experimental and numerical analysis of stone masonry walls strengthened with advanced composite materials*. PhD Thesis. Escuela de Ingeniería de Bilbao, 2009.

[22] Harajli et al. *Static and Cyclic Out-of-Plane Response of Masonry Walls Strengthened Using Textile-Mortar System*. Journal of Materials in Civil Engineering. ASCE/November 2010/1171.

[23] Folk, R.L. Petrology of Sedimentary Rocks. 1974, Hemphills, Texas, USA.

[24] Oliveira D., Lemos C. and Lourenço P.B. (2009). *Masonry arch bridges in the Northwest of Iberian Peninsula: from geometrical issues to load carrying capacity*. REHABEND 2009. Tecnología de la rehabilitación y gestión del patrimonio construido. 29-30 octubre 2009, Bilbao. ISBN 978-84-8873-404-4.

[25] Martín-Caro J.A. (2001). *Análisis estructural de puentes arco de fábrica. Criterios de Comprobación*. PhD Thesis of structural analysis of masonry arch bridges. Polytechnic University of Civil Engineering of Madrid.

[26] Heyman J. The masonry arch. Ellis Horwood Limited, 1982.

[27] Di Tommaso A., Focacci F., Mantegazza G., Gatti A. *FRCM vs FRP composites to strengthen RC beams: a comparative analysis*. 8th intenational symposium on fiber-reinforced polymer reinforcement for concrete structures. Patras, July 16-18, 2007.

[28] Hegger J. and Voss S. *Investigations on the bearing behaviour and application potential of textile reinforced concrete*. Engineering Structures 30, 2008; 2050-2056.

Table 1. Technical specifications of the basalt textile used in

Table 1. Technical specifications of the basalt textile used

Density by area[1]	233 g/m^2
Side length of cell	25 mm
Average thickness	
Uniaxial tension [2]	0.0424 mm
Biaxial tension [3]	0.0848 mm
Working temperature rage	-260 ÷ +800 ºC

[1] Density expressed without considering the bitumen that impregnates the basalt fibres

[2] t = 0.5 M / ρr = 0.5 * 233 [g/m^2] / 2.750 [kg/m^3] = 0.0424 mm

[3] t = M / ρr = 233 [g/m^2] / 2.750 [kg/m^3] = 0.0848 mm

Table 2. Mineralogical characterization of the stone and mortar

Table 2. Mineralogical characterization of the stone and mortar joints

Mineral Phase		Specimen	
		Stone	Jointing Mortar
Calcite	$CaCO_3$		••
Kaolinite	$Al_2Si_2O_5(OH)_4$	•	
Quartz	SiO_2	•••••	•••••
Potassium feldspar (Microcline)	$KAlSi_3O_8$	••	••
Portlandite	$Ca(OH)_2$		••
Muscovite	$KAl_2(AlSi_3O_{10})(OH)_2$	••	•
Gypsum	$CaSO_4*H_2O$		•
Ettringite	$Ca_6Al_2(SO_4)_3(OH)_{12}*26H_2O$		•

Table 3. Mineralogical characterization of strengthening mortars

Table 3. Mineralogical characterization of strengthening mortars

Mineral Phase		Specimen			
		M-A Rinzaffo		M-A Strutturale	
		Material powder form	Hardened specimen	Material powder form	Hardened specimen
Calcite	$CaCO_3$	••	••	••••	•••••
Quartz	SiO_2	•••••	•••••	•••••	••••
Epidote	$Ca_2FeAl_2Si_3O_{12}(OH)$		•		
Ettringite	$Ca_6Al_2(SO_4)_3(OH)_{12}*26H_2O$				•
Potassium feldspar (Microcline)	$KAlSi_3O_8$	••	•	••	•
Sodium Feldspar (albite)	$NaAlSi_3O_8$	••	••	••	•
Portlandite	$Ca(OH)_2$	••	••		
Gypsum	$CaSO_4*H_2O$			•	
Zeolite (gismondite)	$CaAl_2Si_2O_8*4H_2O$	••	••		

Table 4. Physical analysis of the materials

Table 4. Physical analysis of the materials

Mortar type	Density [Kg/m^3]	Absorption by capillarity [Kg/m^2 min-$^{1/2}$]	Absorption under atmospheric pressure %	Water vapour permeability [Kg/m s Pa]	Porosity %	Average pore size Ø [µm]	Pore size distribution
Sandstone	2011	1.48	6.5	-	20.4	28	Unimodal with asymmetry (lowest values)
Jointing Mortar	1625	1.74	-	-	34.1	-	
M-A Rinzaffo	1880	0.18	11.69	2.97E-12	26.44	0.05	Bimodal. Two-pore families. Average size of 0.75 and 0.04 µm.
M-A Strutturale	2060	0.36	15.79	2.07E-12	29.92	0.04	Unimodal.

Table 5. Average values for mechanical test results of materials

Table 5. Average values for mechanical test results of materials

	f_{cm} [MPa]		f_{tm} [MPa]		E [GPa]	
Sandstone	21.3	(0.19)	1.36	(0.13)	5.94	(0.14)
Jointing mortar	2.03	(0.007)	0.98	(0.1)	5.04	(-)
Base mortar	12.6	(0.03)	1.9	(0.04)	7.19	(0.09)
Matrix mortar	21.0	(0.04)	3.5	(0.1)	15.65	(0.027)

Coefficient of variation between brackets

Table 6. Textile tensile test results

Table 6. Textile tensile test results

Specimen type	f_f [N]	σ_f [MPa]	f_f [N/roving]	f_f [mN/Tex]	f_f [kN/m]	$e(f_f)$	E_f [GPa]
TL1	1240	1170	1240	417	50	0.0224	56
TL2	2693	1101	1347	453	54	0.0292	49
TL4	3790	894	948	319	38	0.0218	52
TT4	2849	631	712	240	29	0.0238	43

TL1: mean value from 10 tests TL2: mean value from 5 tests
TL4: mean value from 10 tests TT4: mean value from 9 tests
Resistance expressed as mN/tex is used in industry specifications on fibre textiles. It represents the supported mili-Newtons by the weight in grams of 1000 metres of the fibre yarn
Tensile results were obtained for an equivalent section of 1.06 mm^2 per strand.

Table 7. Summary of experimental test results

Table 7. Summary of experimental test results

Specimen	Maximum Load [kN]		Load Point Displacement at Maximum Load [mm]		Failure Mode
A1	0.98	(1.24) CV: 0.16	2.46	(2.45)	Mechanism
A2	1.30		3.86		Mechanism
A3	1.45		1.04		Mechanism
EX1	19.30	(16.26) CV: 0.17	13.50	(8.79)	Mechanism
EX2	16.83		7.14		BTRM debonding
EX3	12.65		5.73		Masonry crushing

Average value is shown in brackets
CV: Coefficient of Variation

Figure 1. Petrographic analysis of the sandstone. Macroscopic (l

Click here to download high resolution image

Figure 1. Petrographic analysis of the sandstone. Macroscopic (l
Click here to download high resolution image

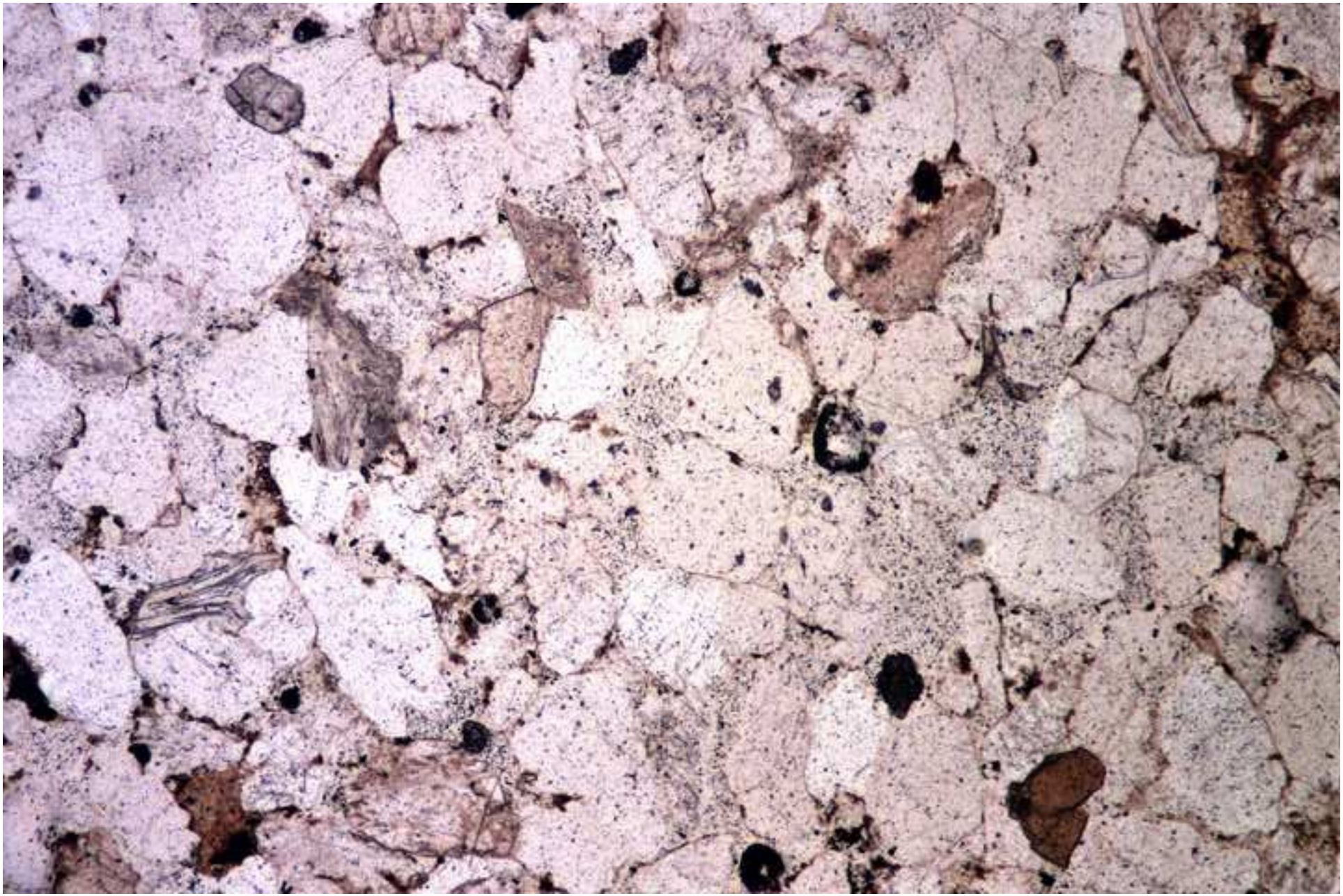

Figure 2. Pure tensile tests of several basalt textile specimens
Click here to download high resolution image

Figure 2. Pure tensile tests of several basalt textile specimens
Click here to download high resolution image

Figure 2. Pure tensile tests of several basalt textile specimens
Click here to download high resolution image

Figure 3. Preparation and testing of the TRM specimens
Click here to download high resolution image

Figure 3. Preparation and testing of the TRM specimens
Click here to download high resolution image

Figure 4. Textile stress-strain curves: two-ply specimen (TRMA)
Click here to download high resolution image

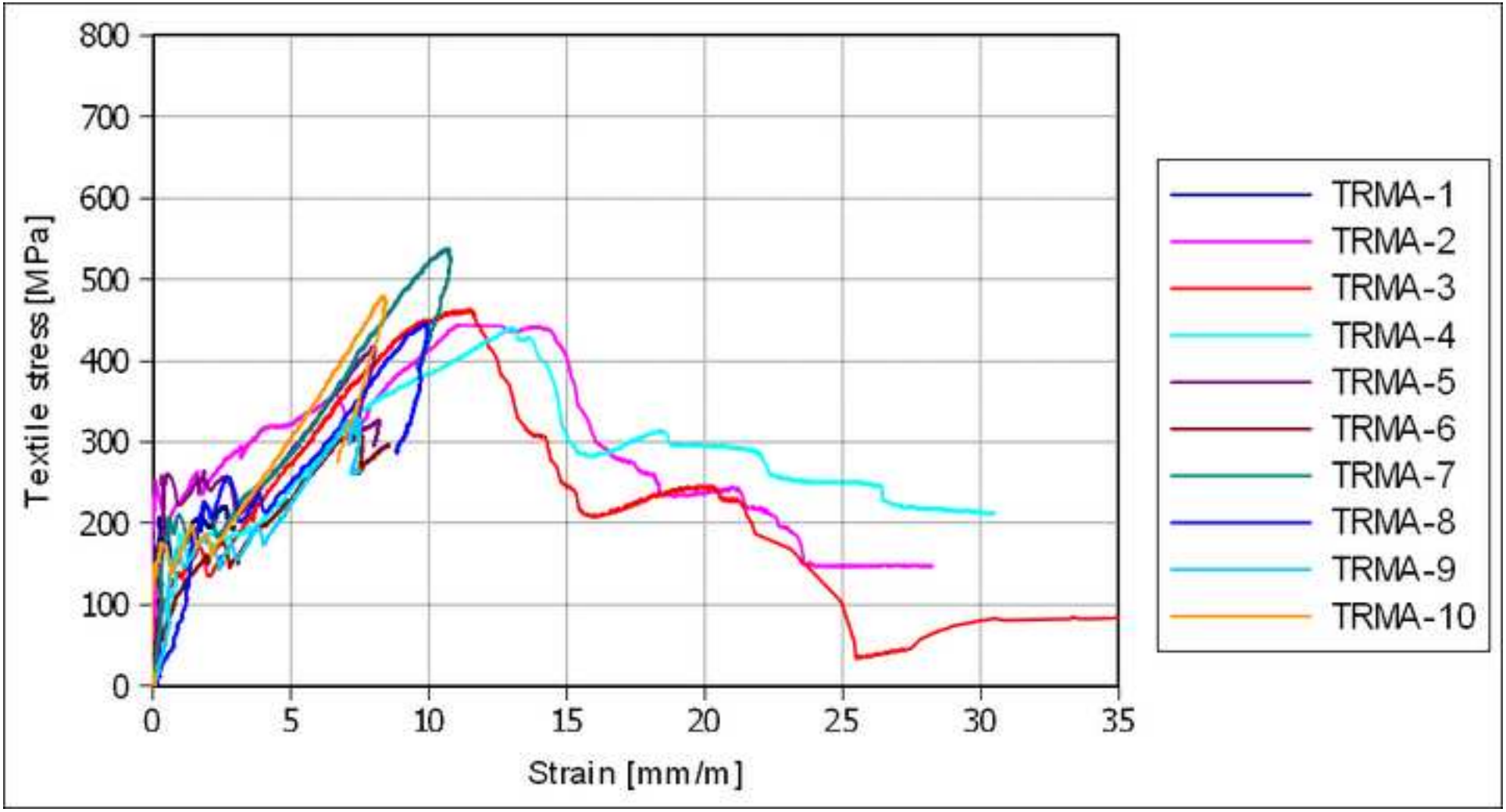

Figure 5. Textile stress-strain curves: two-ply specimen (TRMB)
Click here to download high resolution image

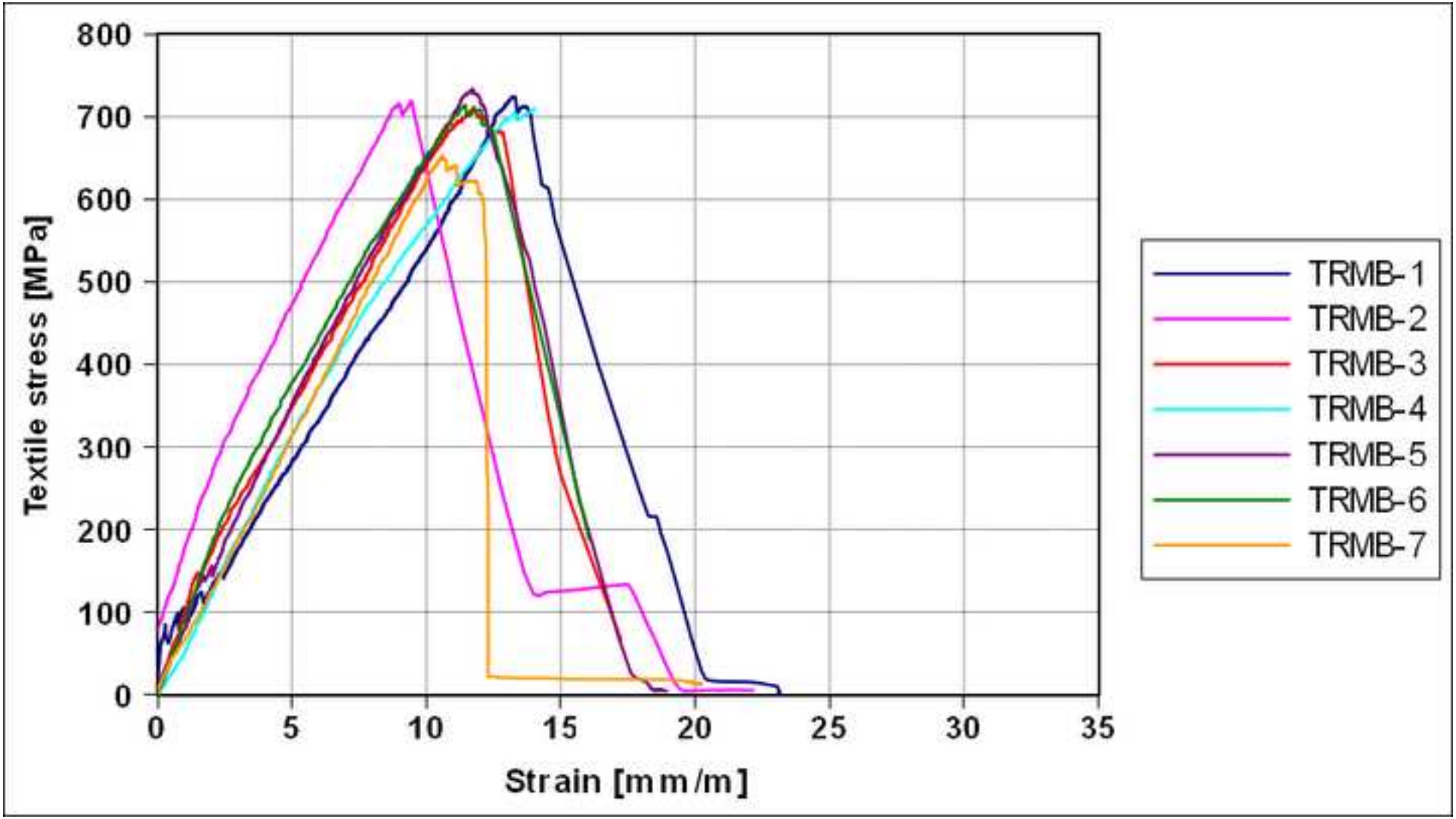

Figure 6. Geometry of the arches

Click here to download high resolution image

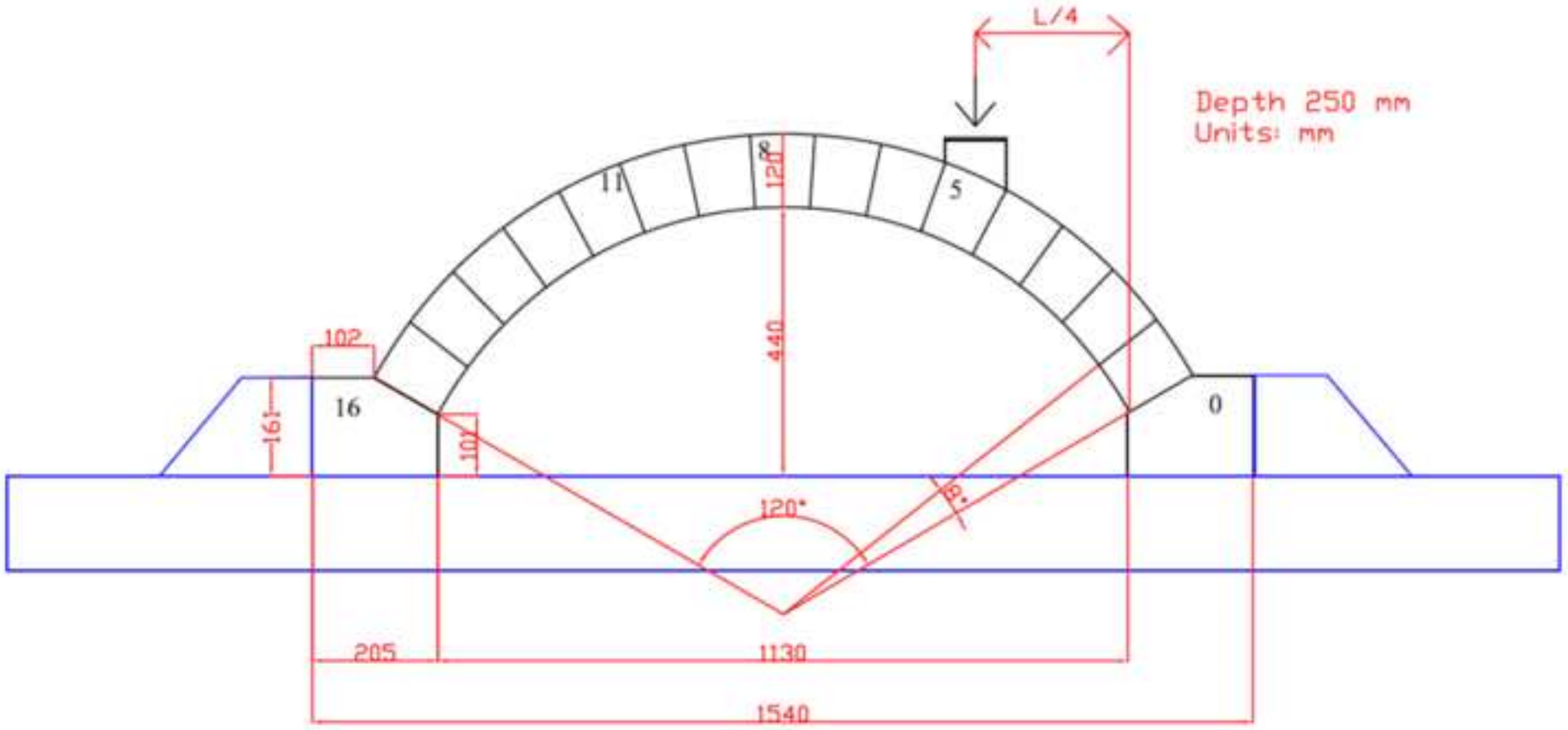

Figure 7. Spike anchors location (left) and strengthening of mas

Click here to download high resolution image

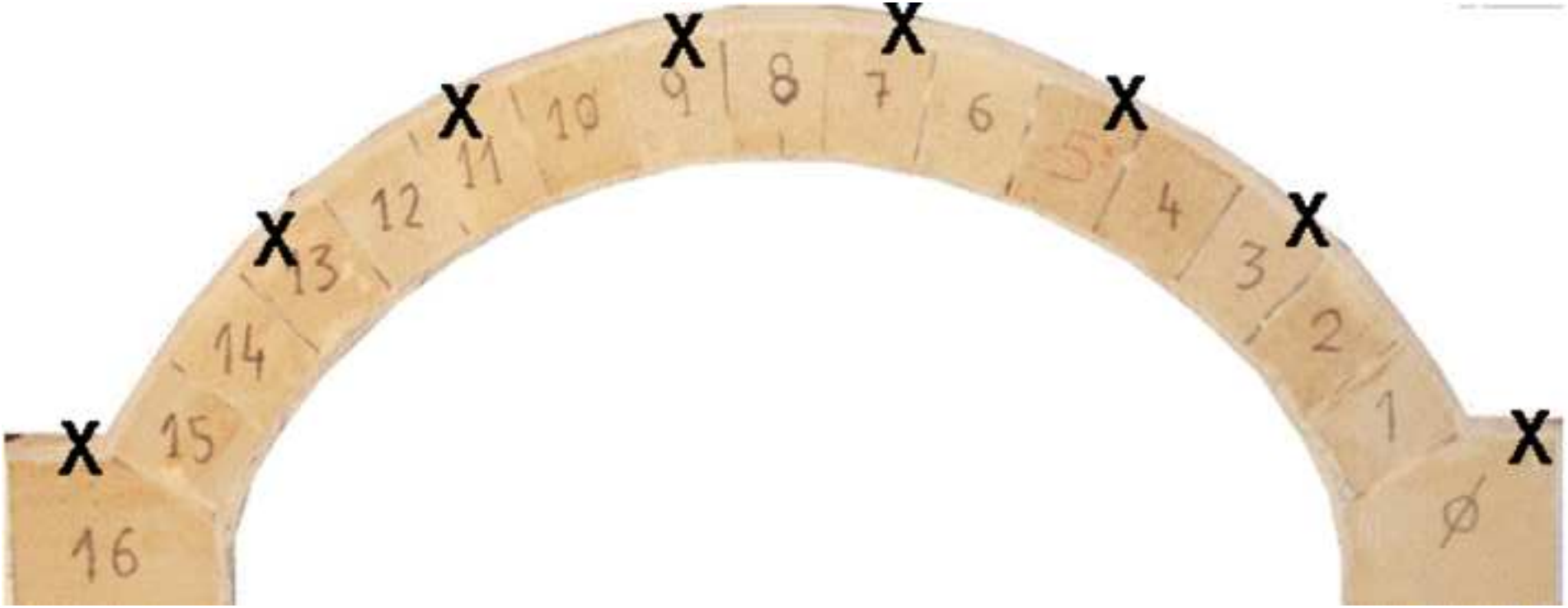

Figure 7. Spike anchors location (left) and strengthening of mas
Click here to download high resolution image

Figure 8. Load-Displacement of load application point for non-st
Click here to download high resolution image

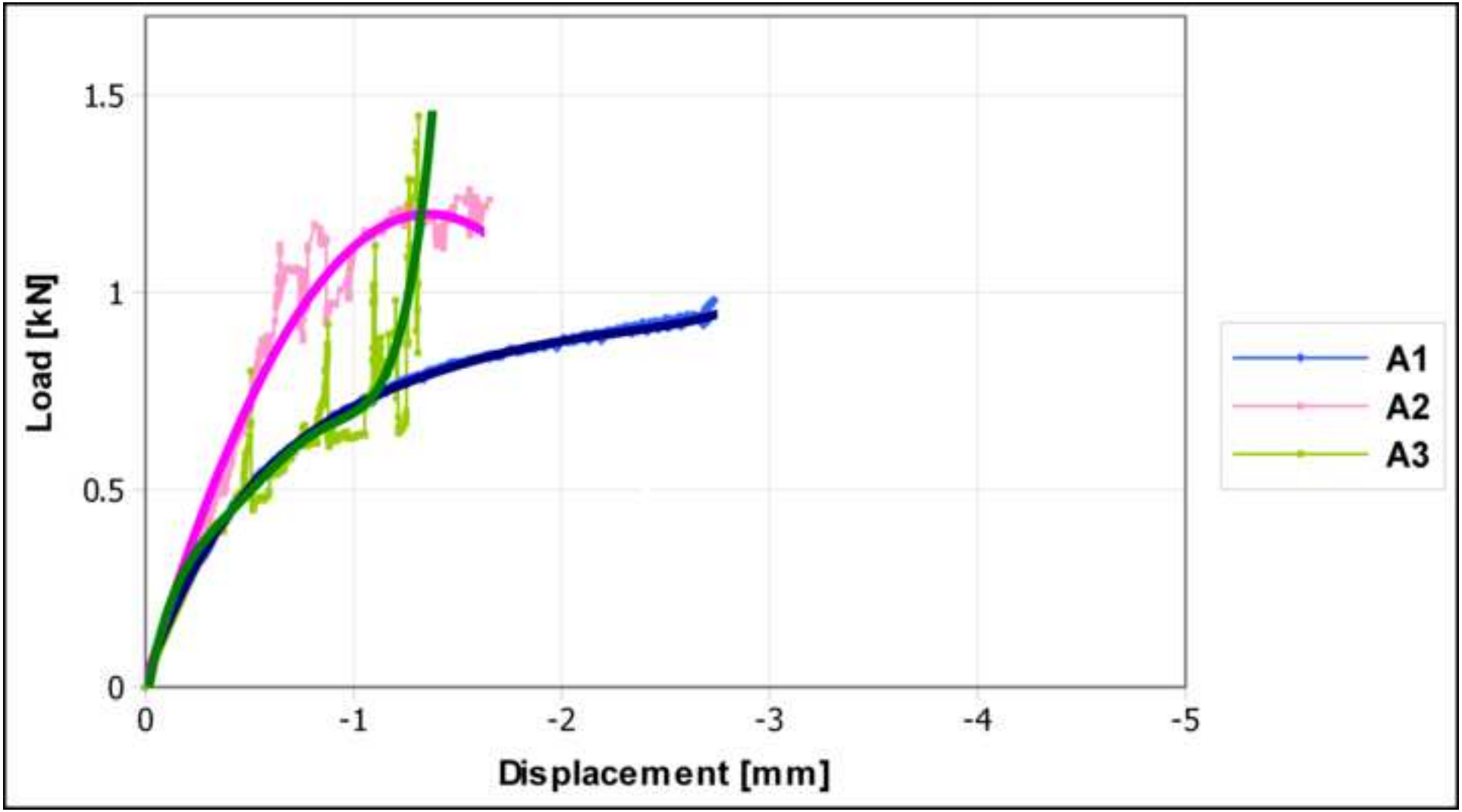

Figure 9. Comparison of the displacement of the left and right h

Click here to download high resolution image

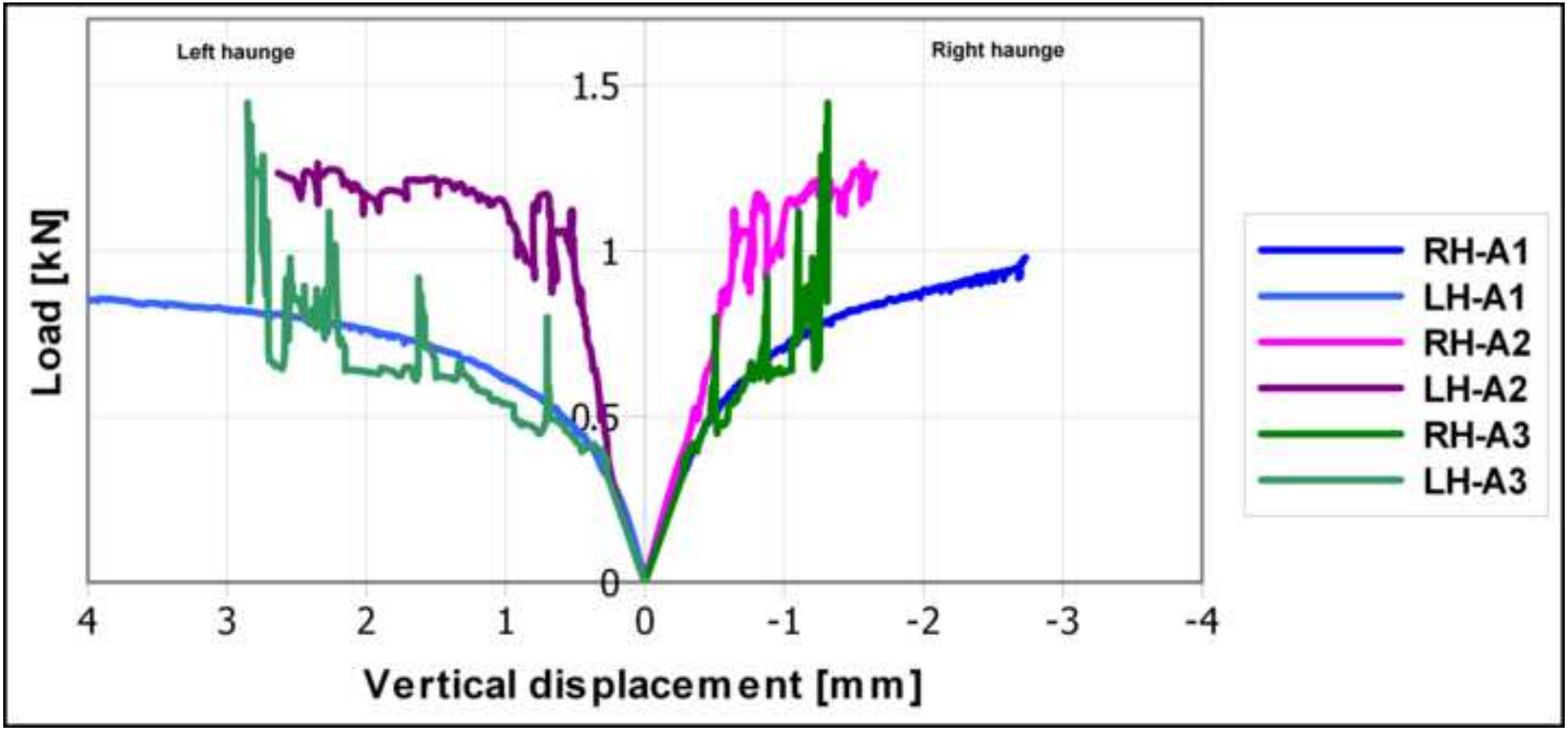

Figure 10. Location and order of appearance of the hinges on non
Click here to download high resolution image

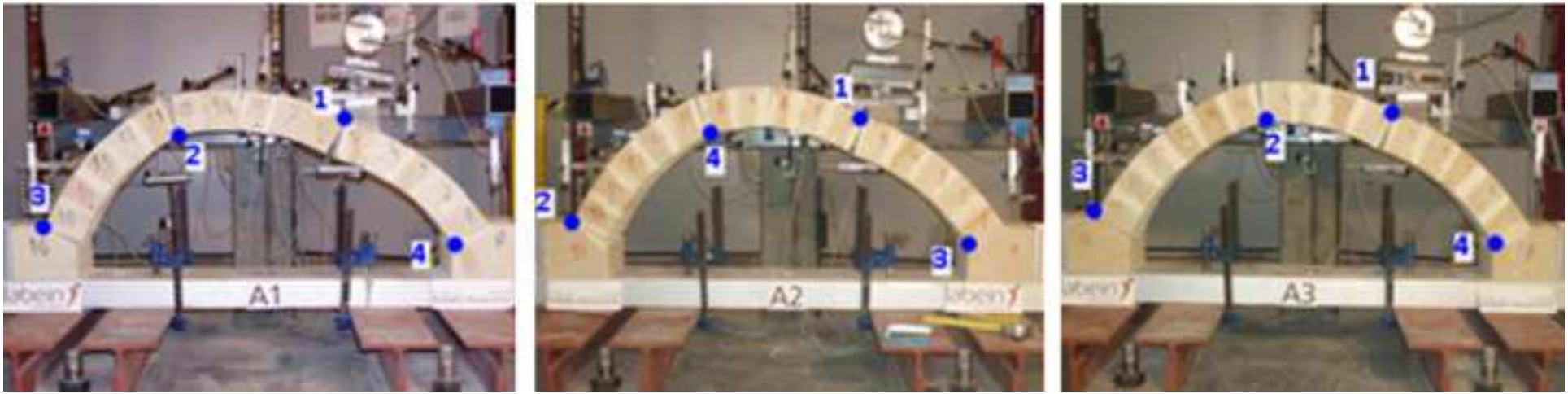

Figure 11. Load/Displacement of load application point for arche
Click here to download high resolution image

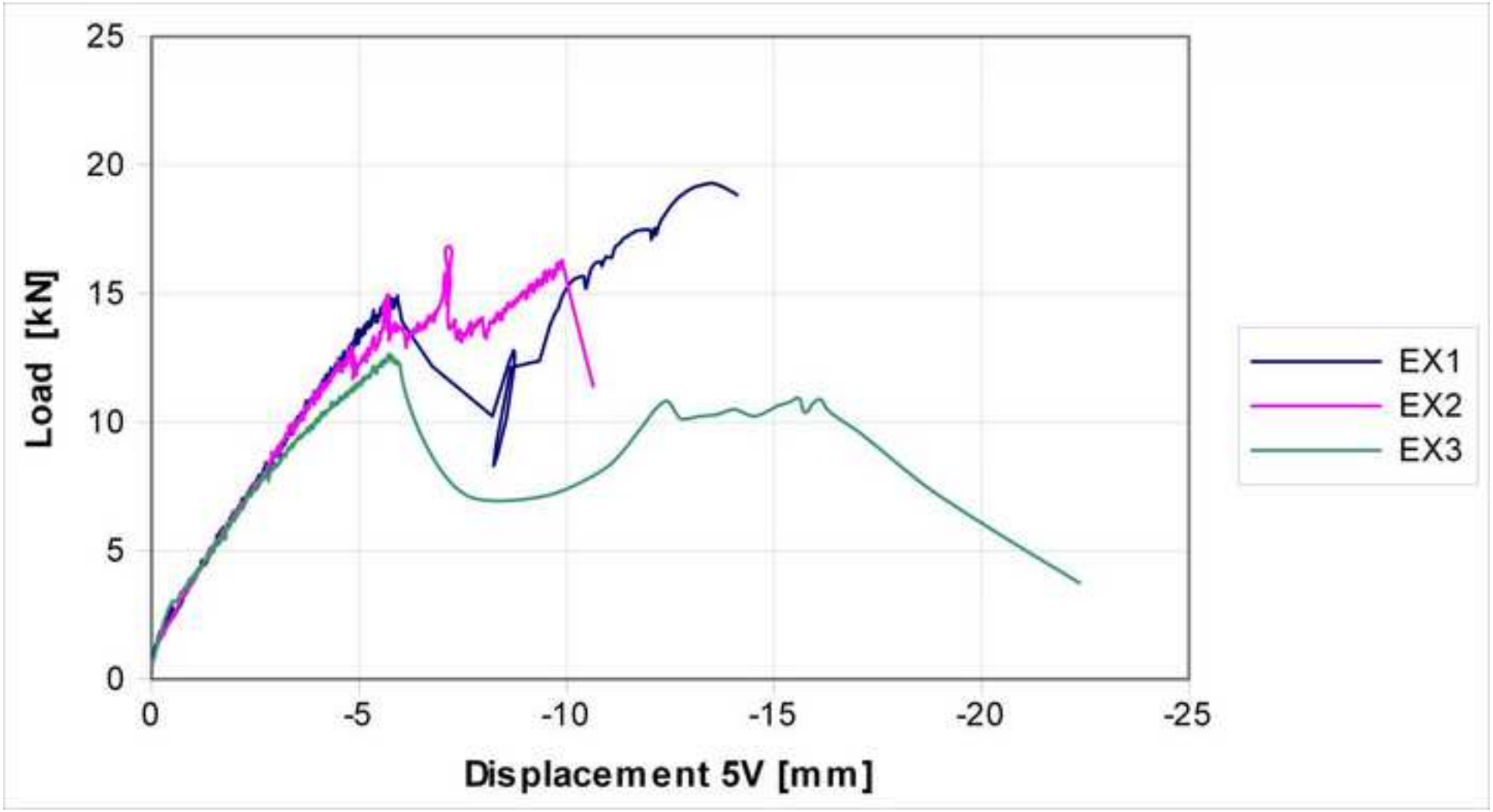

Figure 12. Location and order of appearance of the hinges on arc
Click here to download high resolution image

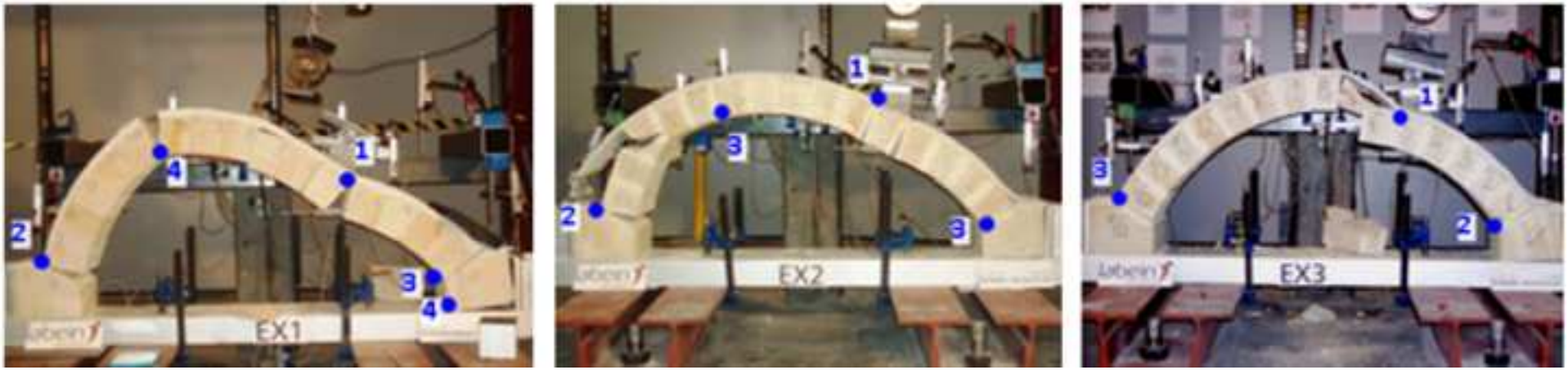

Figure 13. Detailed photographs of arch EX2
Click here to download high resolution image

Figure 13. Detailed photographs of arch EX2
Click here to download high resolution image

Figure 13. Detailed photographs of arch EX2
Click here to download high resolution image